Boffin Access

Open Access Journal | Volume: 2.1

Journal of Water Technology and Treatment Methods

ISSN 2517-7427

Copper Recovery from Industrial Wastewater Using DMSA Coated Magnetic Nanoparticles

Jonathan A Brant*
Adam E Marsh
Savannah Bachman

[1]Department of Civil and Architectural Engineering, University of Wyoming, Laramie, Wyoming, United States

Abstract

Industrial wastewaters are a rich source of valuable materials including rare earth metals like copper. Recovering these resources is difficult because of their dilute concentration and the complex nature of wastewater. This investigation examined the synthesis and performance of dimercaptosuccinic acid (DMSA)-coated maghemite nanoparticles for removing copper from aqueous media. The DMSA-coated nanoparticles achieved apparent adsorption capacities ranging from 2 to 300 mg/g. Apparent adsorption increased with solution pH and ionic strength. This was attributed to the development of more favorable electrostatic conditions between the carboxylate groups on the DMSA molecule and copper with increasing pH. Copper hydroxide precipitation at pH ≥ 7 also influenced copper removal due to enmeshment of the maghemite nanoparticles into the precipitate structure and subsequent removal upon the application of a magnetic field. Copper removal thus increased as copper solubility decreased and/or through the aggregation of precipitates with increasing solution ionic strength. The presence of calcium and magnesium in solution did not reduce copper adsorption under conditions representative of a copper plating wastewater.

Keywords

Maghemite; Nanoparticle; Copper; Adsorption; Wastewater resource recovery

Introduction

Industrial wastewater, including metal finishing and oil and gas produced waters, are potentially lucrative sources of precious metals and other valuable elements. One such metal is copper, whose value in 2018 was approximately $6/kg. Copper concentrations can be relatively high for a variety of industrial flows. For example, copper plating wastewater may contain between 98 to 1,000 mg/L of copper [1-3], while mine drainage can contain between 231 to 1,400 mg/L of copper [4,5]. These are important statistics given the widespread use and unit cost of copper. Industrial wastewaters therefore represent a potentially significant source of revenue, in addition to the ancillary benefits associated with resource recovery. Taking advantage of these opportunities requires separation processes capable of economically recovering these materials from complex mixtures.

Copper recovery from wastewater can be achieved through precipitation of insoluble forms of copper, namely $Cu(OH)_x$ and $Cu_x(CO_3)_x$ [6]. Copper solubility is highly dependent upon pH, being soluble at pH<7 and insoluble at pH≥8 [7]. Although precipitation is an effective copper recovery technique, the purity of the precipitate is highly variable and may contain other metals that were present in solution. For this reason, a number of efforts have focused on developing copper adsorbents for wastewater applications. Adsorbents that have been studied thus far have included fly ash [8], sawdust [9], activated carbon [10], and peat [11]. Recently, the adsorption of copper by surface functionalized nanoparticles (NPs) has become a topic of interest because of their characteristically high specific surface areas and the relative ease with which their respective surface chemistries may be modified.

Super paramagnetic NPs present a unique opportunity to recover valuable resources from wastewater without the aid of traditional solid-liquid separation techniques. Maghemite (γ-Fe_2O_3), the reduced form of magnetite (Fe_3O_4), is a paramagnetic material that has received widespread interest for water treatment applications [12-17]. NP surface coatings are advantageous for metal recovery as adsorption occurs through ionic bonds, rather than covalent bonds as is the case for bare γ-Fe_2O_3, allowing for the metals to desorb from the adsorbent [18]. Dimercaptosuccinic acid (DMSA) is one coating agent that has been evaluated for creating nano-adsorbents. The free carboxylate moieties on the DMSA molecule complex with metals, which can then be neutralized by acidifying the solution [19]. Warner et al. [16] and Yantasee et al. [17] investigated the adsorption of heavy metals, including copper, by DMSA-coated Fe_3O_4 NPs. The DMSA coating increased copper adsorption from synthetic groundwater and river water from 3.45 mg/g for bare

Article Information

DOI: 10.31021/jwt.20192123
Article Type: Research Article
Journal Type: Open Access
Volume: 2 **Issue:** 1
Manuscript ID: JWT-2-123
Publisher: Boffin Access Limited

Received Date: 04 October 2018
Accepted Date: 29 Apr 2019
Published Date: 30 Apr 2019

*Corresponding author:

Jonathan A Brant, PE, PhD
Department of Civil and Architectural Engineering, University of Wyoming
1000 E. University Avenue, Laramie, WY 82071 , United States
Tel: (307)766–5446
E-mail: jbrant1@uwyo.edu

Citation: Brant JA, Marsh AE, Bachman S. Copper recovery from industrial waste water using dmsa coated magnetic nanoparticles. J Water Technol Treat Methods. 2019 Apr ;2(1):123

Copyright: © 2019 Brant JA, et al. This is an open-access article distributed under the terms of the Creative Commons Attribution 4.0 international License, which permits unrestricted use, distribution, and reproduction in any medium, provided the original author and source are credited.

Fe_2O_4 to 36.49 mg/g and 23.82 mg/g, respectively. Similarly, DMSA-coated γ-Fe_2O_3 NPs adsorbed 42.5 mg Pb/g, while bare γ-Fe_2O_3 NPs adsorbed 6.9 mg Pb/g [16]. Singh et al. [18] found that copper adsorption to DMSA-coated Fe_3O_4 NPs increased with solution pH and was completely removed at pH ≥ 6 [18]; however, the impact that copper precipitation may have had on adsorption efficiency was not addressed in this study.

Metal adsorption has been found to increase with increasing solution pH [20-22], NP (adsorbent) concentration [18], and target metal (adsorbate) concentration [20,22]. Conversely, it was found to be inversely proportional to solution ionic strength [20,22]. This has been attributed to competition between the target adsorbate and other cations for adsorption sites, decreased metal activity, and reductions in surface area available for adsorption from NP aggregation [21,22]. The properties of DMSA responsible for increasing metal adsorption are attributed to the increased number of sites onto which metal complexation can occur and increased NP surface area resulting from improved particle stability under a given solution chemistry [13,23]. Clarifying the roles played by copper precipitation and NP aggregation on copper recovery using nano-adsorbents is thus needed to continue the development of this process.

The adsorption of copper from complex media using DMSA-coated γ-Fe_2O_3 NPs was studied to address the aforementioned open questions. The complex media was made to represent wastewater from a metal plating facility based on water quality data reported in the literature. The presence, or absence, of insoluble copper hydroxide, and its impact on the apparent adsorption capacity of the DMSA-coated γ-Fe_2O_3 NPs was quantified.

Experimental Protocols

Chemicals and Reagents

All solutions were made using ultrapure water having a resistivity of 18 MΩ.cm and an unbuffered pH of 7.5. Solution ionic strength was adjusted using sodium chloride (Fisher Scientific, Fair Lawn, NJ) having a purity ≥ 99%. Solution pH was adjusted using either hydrochloric acid (HCl) or sodium hydroxide (NaOH). Both the acid and base were acquired from Fisher Scientific (Fair Lawn, NJ) and had reported purities that were ≥ 99%.

Synthesis of DMSA-Coated γ-Fe_2O_3 NPs

Maghemite NPs (purity ≥ 99.5%) were purchased from U.S. Research Nanomaterials, Inc. (Houston, TX) and used without further purification. The NPs had a measured mean diameter of 28 ± 8.3 nm and a specific gravity of 4.86. The size of the NPs was selected for study to ensure that they were at, or near, maximum magnetic saturation [24]. The γ-Fe_2O_3NPs were coated with DMSA according to the method developed by Auffan et al. [25]. DMSA, having a reported purity ≥ 98% was purchased from Acros Organics (Fair Lawn, NJ) and stored in a brown glass container until used. In a 500 mL glass jar, 400 mg of γ-Fe_2O_3 NPs was dispersed in 400 mL of ultrapure water adjusted to pH 2.75 with 6 N HCl. To create a well dispersed γ-Fe_2O_3 NP suspension, the NPs were sonicated for 30 mins at 30% amplitude by a probe sonicator (Fisher Scientific Sonic Dismembrator Model 500, Fair Lawn, NJ). Following sonication, the pH of the suspension was verified to be 2.75 and, if needed, adjusted back to this value with 6 N HCl or 10 N NaOH. Next, the sealed container was bath sonicated for 1 hr (Branson Model 2510, Danbury, CT) and then probe sonicated for an additional 30 mins at 30% amplitude. Then, 56 mg of DMSA was added to 75 mL of doubly deionized water in a 100 mL glass beaker and the pH was adjusted to 2.75 with 10 N NaOH. The solution pH was verified after 30 mins of mixing and, if needed, was adjusted back to pH 2.75. Immediately after sonication, 73.1 mL of the DMSA solution was added to the γ-Fe_2O_3 NP suspension to create a 6% DMSA:Fe_{total} molar ratio. The DMSA and γ-Fe_2O_3 NP mixture was transferred to a 1 L container and placed on an end-over-end mixer for 24 hrs. After mixing, the pH of the DMSA-coated γ-Fe_2O_3 suspension was adjusted to pH 11 over the course of 1.5 hrs with 10 N NaOH. This facilitated the replacement of ionic bonds between DMSA's carboxylate groups and γ-Fe_2O_3 NPs with covalent bonds between DMSA's thiol groups and oxygen in the γ-Fe_2O_3 NP lattice structure. The solution was returned to the end-over-end mixer for 2 hrs and then acidified to pH 7 for storage. Equally divided into 250 mL plastic bottles, the DMSA-coated γ-Fe_2O_3 NPs were separated from suspension by centrifugation at 22°C for 2 hrs at 16,500 G's. The supernatant was siphoned off, while not disturbing the particle pellet, and then replaced with ultra-pure water. The DMSA-coated γ-Fe_2O_3 NPs were returned to the 1 L glass jar and placed on the end-over-end mixer for 1 hr. In this way, the DMSA-coated γ-Fe_2O_3 NPs were rinsed 5 times with doubly deionized water to remove unbound DMSA from the suspension. After removing the supernatant, the purified DMSA-coated γ-Fe_2O_3 NPs were placed in petri dishes and dried at 45°C. Dehydrated DMSA-coated γ-Fe_2O_3 NPs were scraped from the petri dishes and pulverized with a mortar and pestle and stored in a sealed container at 22°C.

Nanoparticle surface chemistry characterization

Fourier transform infrared spectroscopy (FTIR) measurements were conducted to confirm the surface functionality of the bare and DMSA-coated γ-Fe_2O_3 NPs. A DMSA sample was also characterized, as a reference signature, for comparison to the DMSA-coated NPs. FTIR measurements were done using a Perkin-Elmer Spectrum 1000 FTIR Spectrophotometer. Samples were pulverized and combined with a potassium bromide standard (99.3% purity, Fisher Scientific, Fair Lawn, NJ) to produce a homogenous mixture. The sample constituted 1% of the mixture. IR sample cards were prepared by pressing the sample KBr mixture into a semitransparent pellet on a potassium bromide IR card (International Crystal Labs, Garfield, NJ) using a hydraulic press (Wabash MPI, model 50-18-2TM, Wabash, IN). The slide aperture was uniformly covered with approximately 2 mm of sample and fused into a pellet with 9,500 kgs of force for 60 secs. IR cards were covered top and bottom with aluminum foil to prevent foreign material from contaminating the sample. The potassium bromide background was measured with 225 sub runs to enhance the noise-to-signal ratio. Samples were measured as a ratio to the background slide with 225 sub runs. Measured peaks were matched to their corresponding groups using data reported in the literature.

The mass of DMSA that was adsorbed, or bound, to a unit mass of γ-Fe_2O_3 NPs was determined by X-ray Fluorescence (PANanlytical, model X'Pert PRO, Netherlands). The characteristic wavelengths of iron and sulfur emitted by 3 samples were measured and compared to the magnitude of characteristic radiation emitted by standards of known Fe:S concentration ratios. Without further purification, all of the samples and standards were measured simultaneously and the S:Fe ration in the samples was determined from the standard curve generated during the same measurement cycle.

Nanoparticle size and surface charge

NP size (hydrodynamic diameter, d_h) and size distribution were characterized using dynamic light scattering (Malvern ZetaSizer Nano ZS, Malvern Instruments, Worcestershire, UK). NP size/size distribution was characterized as a function of solution ionic strength (NaCl), ionic composition, and pH in order to determine their physical properties under the same conditions as those used in the adsorption experiments. For all measurements, the NPs were dispersed in a background electrolyte solution at a given pH that had been pre-filtered using a syringe filter having a nominal pore size of 0.20 µm. The presence, and size distribution, of copper hydroxide precipitates was studied as a function of solution pH and I_s using DLS measurements and OLI Electrolyte Simulation Software (OLI Systems, Inc., Cedar Knolls, NJ). Copper solutions having a concentration of 4 mg/L were prepared having a given pH and I_s and allowed to equilibrate for a minimum of 1 hr prior to DLS analysis. The presence, or absence, of precipitates was confirmed through analysis of the resulting size distribution and particle count rate. Turbidity measurements were also done on the samples to support the DLS results. All measurements were compared against theoretical projections from an electrolyte modelling software package (OLI Systems, Inc., Cedar Knolls, NJ).

NP surface charge was characterized in terms of a zeta potential, which was calculated from a measured electrophoretic mobility value under a given set of experimental conditions. Electrophoretic mobility was measured using the DLS, and the zeta potential calculated from it using the Smoluchowski approximation. Electrophoretic mobility was measured as a function of solution ionic strength and pH through automatic titration of the test solution using concentrated solutions of sodium chloride, sodium hydroxide, and/or hydrochloric acid. For the pH titration experiments the test solution was titrated from the natural solution pH (6.5) to either an acidic value (pH 3), or to a basic value (pH 9). This was done to avoid over diluting the sample and substantial modification of the solution ionic strength. All size and zeta potential measurements were done at 25°C and the average results calculated from a minimum of triplicate measurements.

Nanoparticle surface area measurements

The specific surface areas of bare and DMSA-coated γ-Fe_2O_3 NPs were measured using a TriStar 3000 BET surface area analyzer (Micrometrics Instrument Corporation, Norcross, GA). Bare NPs were analyzed as supplied by the manufacturer without further preparation. DMSA-coated NPs were dried immediately following synthesis and purification and then pulverized with a ceramic mortar and pestle. NP samples and a carbon black standard were placed in sample tubes and degassed overnight at 80°C under a helium atmosphere. Degassed samples were weighed and placed in the analyzer. Analysis was performed using a 5-point Brunauer–Emmett–Teller (BET) isotherm and was checked for accuracy against the simultaneously measured carbon black standard.

Copper adsorption by DMSA-coated γ-Fe_2O_3 nanoparticles

Separate copper stock solutions were prepared for assessing adsorption as a function of solution pH or ionic strength (I_s). For the pH experiments, a 200 mg/L solution was created by dissolving 480 mg $CuCl_2$•$2H_2O$ in 1 L of ultrapure water that was acidified to pH<2 for storage. For those experiments involving changes in I_s, a 400 mg/L solution was created by dissolving 959 mg $CuCl_2$•$2H_2O$ in 1 L of ultrapure water that was acidified to pH<2 for storage. Stock solutions were kept in brown glass jars and stored at 4°C until used. A liquid to solid ratio of 100,000 (10 mg NPs/L of solution) was selected for the adsorption tests. Tests were done at a copper concentration of 4 mg/L to ensure an excess of copper ions relative to available adsorption sites were present. The DMSA-coated NPs were added to the electrolyte solution of interest and the pH adjusted using hydrochloric acid or sodium hydroxide. The mixture was then bath sonicated for 30 mins to ensure full dispersion of the NPs prior to adding the copper. Immediately after sonication, the copper was added to the DMSA-coated γ-Fe_2O_3 NP suspension and mixed for 2 hrs. After mixing, a 50 mL sample was withdrawn and placed into a polypropylene centrifuge vial, which was subsequently inserted into a Dexter Magnetic Technologies LifeSep 50SX magnetic separator for 30 min. Without removing the centrifuge vial, a sample was siphoned from the center of the vial and transferred to a 20 mL glass vial. The contents of one CuVer 2 powder pillow (Hach, Loveland, CO) were combined with the 10 mL sample and mixed for 30 secs. After 10 mins, a quartz cell was filled with sample and measured against anultrapure water background for absorbance at λ=559 nm using a UV-vis spectrophotometer (Shimadzu UV-1800 Spectrophotometer, Japan).

Copper adsorption was also evaluated in the presence of two competing adsorption cations, calcium and magnesium. The test solution was comprised of the following cations and anions: 0.002 M Cu^{2+}, 0.004 M Ca^{2+}, 0.03 M Mg^{2+}, 0.07 M Na^{+}, 0.012 M SO_4^{2-} and 0.024 M Cl^{-}. The solution composition was based on that reported in the literature for copper plating wastewater [3]. To accurately measure the influence of competitive ions on copper adsorption, it was important that the copper was fully dissolved. Thus, the critical coagulation pH, an indicator of copper solubility, of copper hydroxide was determined using DLS and turbidity measurements. From the DLS measurements, the CC pH of copper in the complex media was determined to be 5.70. This finding was corroborated by the turbidity measurements, in which precipitate formation was detected at pH 5.76. These experimental results were confirmed using an electrolyte modeling software (OLI Systems, Inc., Cedar Knolls, NJ). According to this theoretical assessment, the copper precipitated out as copper(II) hydroxide($Cu(OH)_2$) between pH 5.5 to 6 (Figure 1). Based on these findings, pH 5.40 was selected to prevent the formation of precipitant, $Cu(OH)_2$ during the associated adsorption experiments (Supplementary Figures).

Results and Discussion

Surface chemistry and aggregation state of DMSA-coated γ-Fe_2O_3 nanoparticles

Zeta potential as a function of solution pH (I_s=1 mM) is reported in Figure 2 for the bare and DMSA-coated γ-Fe_2O_3 NPs. The isoelectric point (pH_{iep}) for the bare γ-Fe_2O_3 NPs was pH 6.5; the pH_{iep} for the DMSA coated γ-Fe_2O_3 NPs shifted to pH 2.7. The surface charge for the bare γ-Fe_2O_3 NPs, arises from the coordination by protons and hydroxyl ions [23]. In agreement with this theory, the pH_{iep} of the bare γ-Fe_2O_3 NPs occurred at pH 6.7, where the concentrations of protons and hydroxyl ions is nearly equal. The charge for the DMSA-coated NPs arises from the deprotonation of the carboxylate groups on the DMSA molecule. The pH_{iep} values measured here, agree with those previously reported in the literature for both bare (pH_{iep}=6.3-7.8) [15,26] and DMSA-coated γ-Fe_2O_3 NPs (pH_{iep}<4) [23]. The shift from pH 6.5 to 2.7 indicates that a DMSA-coating was present on the NP surface. DMSA's two carboxylate moieties are characterized by pKa values of 2.7and 3.5. The origin of the further increase in the magnitude of the zeta potential from pH 4 to 6 is unclear; however, it may be attributed to the coordination of hydroxyl ions at uncoated portions of the maghemite surface.

Specific adsorption capacity (mg adsorbate/g adsorbent) is a function of the available surface area of the adsorbent on which adsorption can occur. It is therefore important that the NPs remain in a non-aggregated state to maximize the SSA and in turn the specific adsorption capacity. Aggregation of charged particles is well-established to be a function of solution pH and I_s as these variables affect the sign and magnitude of the electrostatic interactions that dictate colloidal stability [27]. The unmodified γ-Fe_2O_3 NPs aggregated as the solution pH approached the measured pH_{iep} (pH 6.5) for these NPs. At pH 5.7 the bare NPs had a mean number weighted d_h of 942 nm. Moving away from the pH_{iep} in both directions, the mean number weighted d_h for the unmodified γ-Fe_2O_3 NPs decreased, reaching a minimum value of 57 nm at pH 3, where they were strongly positively charged (Figure 2). This suggests that the bare γ-Fe_2O_3 NPs were stabilized through charge-charge interactions. In contrast to the unmodified γ-Fe_2O_3 NPs, the DMSA-coated γ-Fe_2O_3 NPs exhibited a consistent mean number weighted d_h of roughly 65 nm at pH ≥ 5, which was at approximately 2 pH units higher than the measured pH_{iep} for these NPs. Below pH 5, the DMSA-coated γ-Fe_2O_3 NPs aggregated; reaching a maximum number weighted d_h of 730 nm at pH 3. At pH 3 the DMSA-coated NPs were weakly charged (≤ |20mV|). The improvement in stability of the DMSA-coated γ-Fe_2O_3 NPs, relative to the unmodified form, is attributed to enhanced electrosteric interactions resulting from the DMSA surface groups. Note that at pH ≥ 5, the DMSA-coated γ-Fe_2O_3 NPs were strongly charged (>-|30 mV|), while the unmodified NPs were not until approximately pH 8 (Figure 2).

The zeta potential and size data for the DMSA-coated NPs suggest several points that are relevant to their copper adsorption potential. One, they were strongly negatively charged at pH ≥ 4.0, meaning that ionic adsorption/complexation sites were available. Second, the NPs were well-dispersed at pH ≥ 5.0, so they should maintain a consistent SSA over a broad pH range. This latter point neglects, however coagulation that will be induced by the copper as it adsorbs to, and shields, the charge of the DMSA-coated NPs.

Previously, DMSA was reported to form ionic bonds between its thiol groups and the oxygen groups at the surface of the γ-Fe_2O_3 [25]. The detection of carboxylic groups and carbon-carbon double bonds

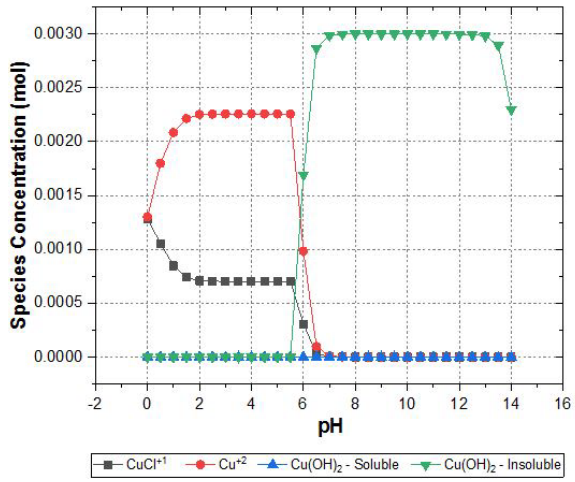

Figure 1: Speciation plot for copper as a function of solution pH in the synthetic plating wastewater (T=25°C)

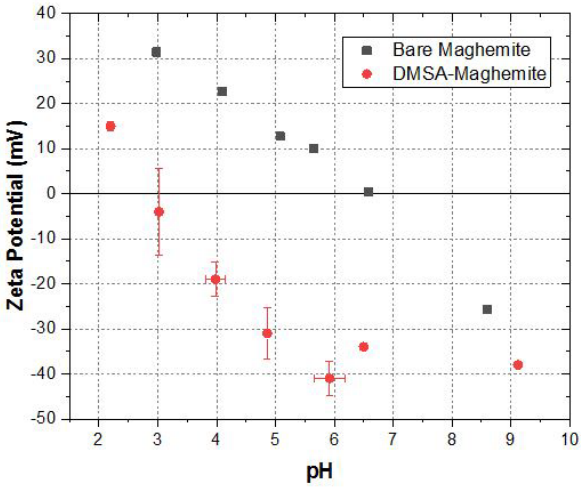

Figure 2: Zeta potential as a function of solution pH for the bare and DMSA-coated γ-Fe_2O_3 NPs (n=10, I_s=1 mM, T=25°C).

at λ = 1620 cm^{-1} and 1410 cm^{-1}, respectively support this structure. No characteristic peaks for thiol groups appear in the FTIR spectra for the coated γ-Fe_2O_3. This indicates that the thiol groups are located within the interior of the coating and are shielded from detection by carboxylate groups located at the exterior of the coating.

The SSA of the unmodified and DMSA-coated γ-Fe_2O_3 NPs were 84.03 ± 0.72 m^2/g and 95.18 ± 0.21 m^2/g, respectively. Thus, the DMSA coating resulted in a 13.3% increase in SSA for the γ-Fe_2O_3 NPs, which is attributed to the reduced aggregation tendency of the surface modified nanoparticles. According to XRF measurements, DMSA was determined to account for 1.26 ± 0.04% of the coated γ-Fe_2O_3 NP mass. From this, the coating density was determined to be 4.4 × 10^{17} DMSA molecules/m^2. The measured SSA of DMSA-coated γ-Fe_2O_3 NPs exceeded the theoretical value of 20 m^2/g, which was based on assumptions of spherical NP geometry and a diameter of 65 nm. This discrepancy may be attributed to the polydisperse nature of the DMSA-coated NP dispersion and/or to the NPs being porous rather than solid spheres.

Copper adsorption

The adsorption capacity of the DMSA-coated γ-Fe_2O_3 NPs for copper was evaluated as a function of solution pH (I_s=10 mM), I_s, and in the presence of competing cations. Copper adsorption increased with pH from 2.4 mg/g at pH 4 to 235 mg/g at pH 8. This increase was attributed to the development of more favorable electrostatic interactions (more attractive) between the copper and the carboxylate groups of the DMSA molecules on the γ-Fe_2O_3 NP surface. The NPs synthesized here achieved adsorptive capacities comparable to Yantasee et al. [17] [19.3 mg/g] and Warner et al. [16] [23.8 mg/g]; however, these literature values were measured at pH 7.8 and copper precipitation was not explicitly investigated. Because DSMA is bound through ionic interactions to the γ-Fe_2O_3 surface through its thiol groups (S-O), carboxylic moieties are free to chelate soft metals. The electronegative groups, whose numbers increase with pH, provide for ionic bonds to be formed with the free copper [20,22]. This scenario was verified through the observed relationship between pH and zeta potential, where it became more negative with increasing solution pH. The decreased proton concentration at higher solution pH values reduce the competition between metals and protons for available adsorption sites [20,22]. Importantly, the relationship between pH and copper adsorption implies that increasing solution acidity may desorb copper. Effective copper desorption would allow for NP regeneration/reuse and copper recovery [20,28].

Interestingly, adsorption continued to increase even after the NP zeta potential plateaued at approximately -40 mV at pH ≥ 6 (Figure 2). At pH ≥ 4 the carboxylate groups should be fully deprotonated (pK_2=3.5); furthermore, any coordinated hydroxyl ions should not act as significant adsorption sites for copper. This indicates that factors beyond increasing electrostatic attraction between the copper and the NPs contributed to the measured adsorption values. Note that the DMSA-coated NPs remained stable at pH ≥ 5 (I_s=10 mM), therefore, changes in SSA would not be a significant factor. Decreasing proton concentrations may enhance copper adsorption by decreasing competition for adsorption sites [29]. Additionally, the formation of insoluble copper hydroxide precipitates at pH>5.4 may have contributed to the increase in the observed copper removal.

Copper solubility is <4 mg/L at pH 7and reaches a minimum solubility of 0.5 mg/L at pH 8 [30]. The presence of the copper(II) hydroxide precipitates was confirmed through DLS measurements (Figure 3a). At pH 7 (I_s=10 mM) the copper solution was characterized by precipitates with a mean intensity weighted d_h of 171 nm with a broad size distribution (Figure 3a). As the solution I_s increased so too did the mean size of the precipitates. Using electrolyte modelling, the solubility point of copper increases from pH 5.4 at 0 mM to pH 6.5 at 100 Mm (Figure 4). At pH 7, the precipitates were characterized by similar size distributions at I_s ≥ 50 mM. At I_s=10 mM the size distribution for the DMSA-coated NPs was characterized by a single peak at 59 nm (Figure 3b). At I_s=50 mM the DMSA-coated NPs were characterized by a bimodal size distribution with peaks at 79 nm and 255 nm. Therefore, the NPs were smaller than the copper hydroxide precipitates irrespective of the solution I_s or pH. The presence of copper hydroxide precipitates means that copper removal can occur through complexation with the carboxylate moieties as well as through physical enmeshment of the NPs into the precipitate structure.

To confirm this hypothesis it was necessary to eliminate any experimental artifacts that may have influenced the copper concentration measurements. Using Stokes Law, the maximum mean settling velocity of the copper(II) hydroxide precipitates was calculated to be 3.09 × 10^{-7} m/s (pH=7, T=25°C, r=232 nm, ρ_p=3370 kg/m^3). From this, their maximum gravitational settling distance during the 30 min magnetic separation process was 0.56 mm. It is important to note that copper is not magnetic and the magnetic field does not affect its settling behavior. Because samples were drawn from approximately 30 mm below the liquid's surface, precipitate settling out of the sampling volume was ruled out as a major contributor.

Interference between the precipitates and the CuVer® 2 colorimetric reagent was ruled out as a consideration because samples were acidified to pH 4.5-5 where copper solubility greatly exceeds 100 mg/L [7]. Therefore, any precipitate initially present in solution was dissolved prior to reaction with the CuVer® 2 reagent

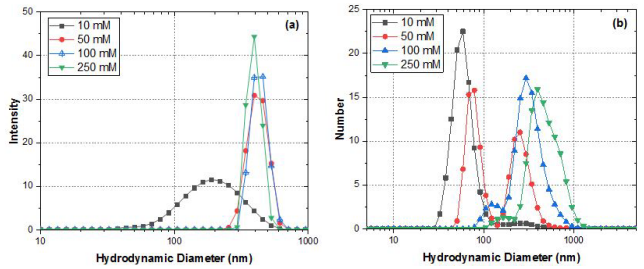

Figure 3: (a) Intensity weighted size distributions for copper hydroxide precipitates as a function of solution ionic strength (pH=7, T=25°C); (b) Number weighted size distributions for the DMSA-coated NPs as a function of solution ionic strength (pH=7, T=25°C).

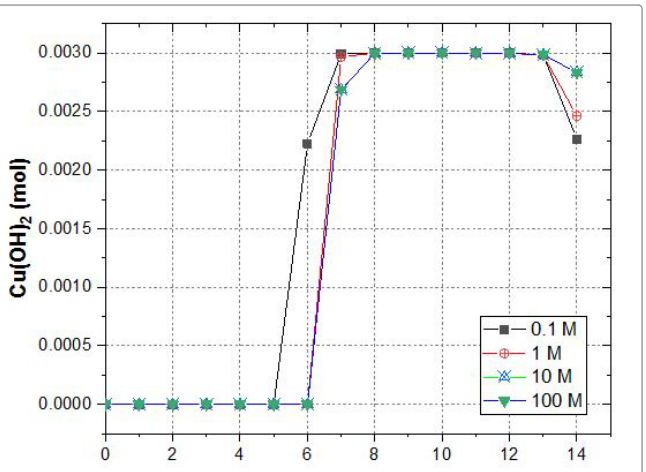

Figure 4: The precipitation point for $Cu(OH)_2$ is shifted from the previously modeled pH 5.75 to pH 6.5 when ionic solution contains 100 molNaCl.

and thus the copper concentration measured after magnetic separation of the DMSA-coated NPs was accurate. Given this, the improvement in copper removal with increasing solution pH was attributed to the DMSA-coated NPs becoming enmeshed within the precipitate structure in addition to the adsorption of free copper ions onto the DMSA molecule. As the solubility of the copper decreases the precipitate size increases resulting in a greater amount of copper being removed per unit mass of NPs. In this way, DMSA-coated NPs removed copper beyond the amount directly bound to the NP surface. Thus, the onset of copper precipitation is important to correctly identifying the removal mechanism. This is important because of the need to avoid the presence of other dissolved metals in the precipitate structure, which would negatively affect the purity of the recovered copper.

Copper adsorption by the DMSA-coated NPs was also evaluated as a function of solution I_s while holding the pH constant at 7.0 (Figure 5). Copper adsorption increased with increasing solution I_s, reaching an approximate maximum of 300 mg/g at I_s=50 mM. This I_s corresponded to the CCC for the copper hydroxide precipitates at pH 7, where they formed a polydisperse suspension having a mean intensity weighted d_h=900 nm (Figure 3). The DMSA-coated NPs also formed a polydisperse suspension irrespective of solution I_s and were characterized by a CCC of roughly 50 mM NaCl at pH 7. Given the polydisperse nature of the DMSA-coated NPs and the copper hydroxide precipitates identifying the exact CCC for these suspension is difficult. Regardless, copper removal seems to reach a maximum near the CCC for both materials. The correlation suggests that the NPs are not solely complexing with free copper ions, but are becoming physically enmeshed in the precipitate structures. This is supported by the similar adsorption values that were measured for the bare

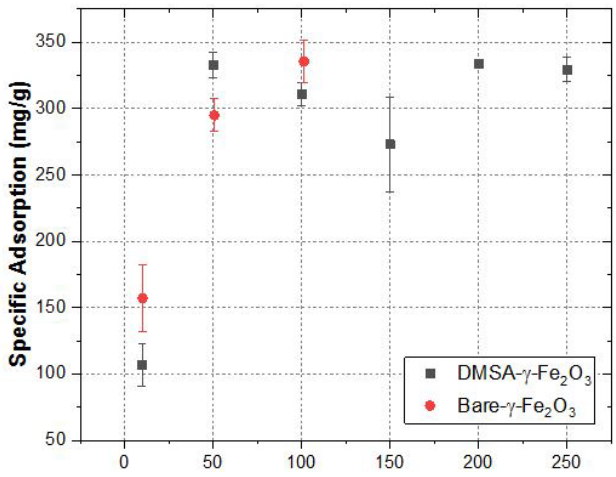

Figure 5: Copper adsorption as a function of solution ionic strength for bare and DMSA-γ-Fe_2O_3 nanoparticles (T=22°C, pH=7).

and DMSA-coated NPs. Thus, under the influence of a magnetic field, the NPs remove entire precipitates, not just the free copper to which the NPs are directly adsorbed (i.e., the DMSA coating plays a less prominent role in the presence of copper precipitates). Separation increases as the size of the precipitates increases through changes in copper solubility (pH) and/or precipitate aggregation from increasing I_s and coagulation from the copper.

The selectivity of DMSA-coated γ-Fe_2O_3 NPs for copper was evaluated using a synthetic copper plating wastewater. A mean copper adsorption value of 21 ± 10 mg/g (n=4) was measured at pH 5.4. This value is statistically the same as that measured in the simple electrolyte solution at the same pH (=23 mg/g). Note that no copper precipitates were detected under these test conditions. Although the copper adsorption would decrease once threshold concentrations for these cations relative to the copper concentration were reached [20], it was not altered in a water representative of an industrial waste stream. This suggests that these adsorbents are, at least under select conditions, feasible for application in real wastewaters.

Summary

DMSA-γ-Fe_2O_3 NPs were successfully synthesized and used to remove dissolved and insoluble forms of copper from solution. The DMSA coating improved NP stability as a function of solution pH and I_s. Apparent copper adsorption ranged from 2 to 300 mg/g and increased with solution pH and I_s at pH 7. The onset of copper hydroxide precipitation, and subsequent aggregation of the precipitates, greatly affected the apparent adsorption of copper to the coated NPs. Dissolved copper and the precipitates were removed from solution *via* complexation with the carboxylate groups on the DMSA molecule and physical enmeshment of the NPs into the precipitate structure. Adsorbent-adsorbate complexes were removed from suspension through application of a magnetic field demonstrating the viability of these adsorbents for use in practical applications.

Acknowledgements

We gratefully acknowledge funding for this study that was provided by the Wyoming NASA Space Grant Consortium (Grant # NNX10AO95H) and the Partner University Fund (Puf). We would also like to thank Dr. Jerome Labille and Dr. Melanie Auffan of the Centre Européen de Recherche et d'Enseignement des Géosciences de l'Environnement (CEREGE, Aix en Provence) for their assistance with the characterization and synthesis of the maghemite nanoparticles.

References

1. Kadirvelu K, Thamaraiselvi K, Namasivayam C. Removal of heavy metals from industrial wastewaters by adsorption onto activated carbon prepared from an agricultural solid waste. Bioresour Technol. 2001 Jan;76(1):63-65.

2. Periasamy K, Namasivayam C. Removal of Nickel(Ii) from Aqueous-Solution and Nickel-Plating Industry Waste-Water Using an Agricultural Waste-Peanut Hulls. Waste Manage. 1995;15(1):63-68.
3. Venkateswaran P, Navaneetha Gopalakrishnan A, Palanivelu K. Di(2-ethylhexyl)phosphoric acid-coconut oil supported liquid membrane for the separation of copper ions from copper plating wastewater. J Environ Sci (China). 2007;19(12):1446-1453.
4. Petrov S, Nenov V. Removal and recovery of copper from wastewater by a complexation-ultrafiltration process. Desalination. 2003;162:201-209.
5. Valenzuela F, Basualto C, Tapia C, Sapag J. Application of hollow-fiber supported liquid membranes technique to the selective recovery of a low content of copper from a Chilean mine water. J Membrane Sci. 1999;155(1):163-168.
6. Sun JM, Shang C, Huang JC. Co-removal of hexavalent chromium through copper precipitation in synthetic wastewater. Environ Sci Technol. 2003 Sep;37(18):4281-4287.
7. Powell KJ, Brown PL, Byrne RH, Gajda T, Hefter G, et al. Chemical speciation of environmentally significant metals with inorganic ligands Part 2: The Cu2+-OH-, Cl-, CO32-, SO42-, and PO43- systems - (IUPAC technical report). Pure Appl Chem. 2007;79(5):895-950.
8. Gupta VK, Ali I. Utilisation of bagasse fly ash (a sugar industry waste) for the removal of copper and zinc from wastewater. Sep Purif Technol. 2000;18(2):131-140.
9. Yu B, Zhang Y, Shukla A, Shukla SS, Dorris KL. The removal of heavy metal from aqueous solutions by sawdust adsorption - removal of copper. J Hazard Mater. 2000 Dec;80(1-3):33-42.
10. Monser L, Adhoum N. Modified activated carbon for the removal of copper, zinc, chromium and cyanide from wastewater. Sep Purif Technol. 2002;26(2-3):137-146.
11. Brown PA, Gill SA, Allen SJ. Metal removal from wastewater using peat. Water Res. 2000;34(16):3907-3916.
12. Afkhami A, Norooz-Asl R. Removal, preconcentration and determination of Mo(VI) from water and wastewater samples using maghemite nanoparticles. Colloid Surface A. 2009;346(1-3):52-57.
13. Auffan M, Rose J, Proux O, Borschneck D, Masion A, et al. Enhanced adsorption of arsenic onto maghemites nanoparticles: As(III) as a probe of the surface structure and heterogeneity. Langmuir. 2008 Apr;24(7):3215-3222.
14. Chowdhury SR, Yanful EK. Arsenic and chromium removal by mixed magnetite-maghemite nanoparticles and the effect of phosphate on removal. J Environ Manage. 2010 Nov;91(11):2238-2247.
15. Hu J, Chen G, Lo IM. Removal and recovery of Cr(VI) from wastewater by maghemite nanoparticles. Water Res. 2005 Nov;39(18):4528-4536.
16. Warner CL, Addleman RS, Cinson AD, Droubay TC, Engelhard MH, et al. High-performance, superparamagnetic, nanoparticle-based heavy metal sorbents for removal of contaminants from natural waters. ChemSusChem. 2010 Jun;3(6):749-757.
17. Yantasee W, Warner CL, Sangvanich T, Addleman RS, Carter TG, et al. Removal of heavy metals from aqueous systems with thiol functionalized superparamagnetic nanoparticles. Environ Sci Technol. 2007 Jul;41(14):5114-5119.
18. Singh S, Barick KC, Bahadur D. Surface engineered magnetic nanoparticles for removal of toxic metal ions and bacterial pathogens. J Hazard Mater. 2011 Sep;192(3):1539-1547.
19. Desiraju GR. C-H...O and other weak hydrogen bonds. From crystal engineering to virtual screening. Chem Commun (Camb). 2005 Jun;(24):2995-3001.
20. Dahiya S, Tripathi RM, Hegde AG. Biosorption of lead and copper from aqueous solutions by pre-treated crab and arca shell biomass. Bioresource Technol. 2008;99(1):179-187.
21. Das N. Recovery of precious metals through biosorption-A review. Hydrometallurgy. 2010;103(1-4):180-189.
22. Reddad Z, Gerente C, Andres Y, Le Cloirec P. Adsorption of several metal ions onto a low-cost biosorbent: Kinetic and equilibrium studies. Environ Sci Technol. 2002;36(9):2067-2073.
23. Fauconnier N, Pons JN, Roger J, Bee A. Thiolation of maghemite nanoparticles by dimercaptosuccinic acid. J Colloid Interf Sci. 1997;194(2):427-433.
24. Coey JMD. Noncollinear Spin Arrangement in Ultrafine Ferrimagnetic Crystallites. Phys Rev Lett. 1971;27(17):1140.
25. Auffan M, Decome L, Rose J, Orsiere T, De Meo M, et al. In vitro interactions between DMSA-coated maghemite nanoparticles and human fibroblasts: A physicochemical and cyto-genotoxical study. Environ Sci Technol. 2006 Jul;40(14):4367-4373.
26. Fauconnier N, Bee A, Roger J, Pons JN. Synthesis of aqueous magnetic liquids by surface complexation of maghemite nanoparticles. J Mol Liq. 1999;83(1-3):233-242.
27. Chen KL, Mylon SE, Elimelech M. Influence of solution chemistry on the aggregation kinetics of alginate-coated hematite colloids. Abstr Pap Am Chem S. 2005;229:U647-U647.
28. Gupta R, Ahuja P, Khan S, Saxena RK, Mohapatra H. Microbial biosorbents: Meeting challenges of heavy metal pollution in aqueous solutions. Curr Sci India. 2000;78(8):967-973.
29. Saad R, Belkacemi K, Hamoudi S. Adsorption of phosphate and nitrate anions on ammonium-functionalized MCM-48: effects of experimental conditions. J Colloid Interface Sci. 2007 Jul;311(2):375-381.
30. Paulson A, Kester D. Copper(II) ion hydrolysis in aqueous solution. Journal of Solution Chemistry. 1979;9(4):269-277.

Supplementary Figures

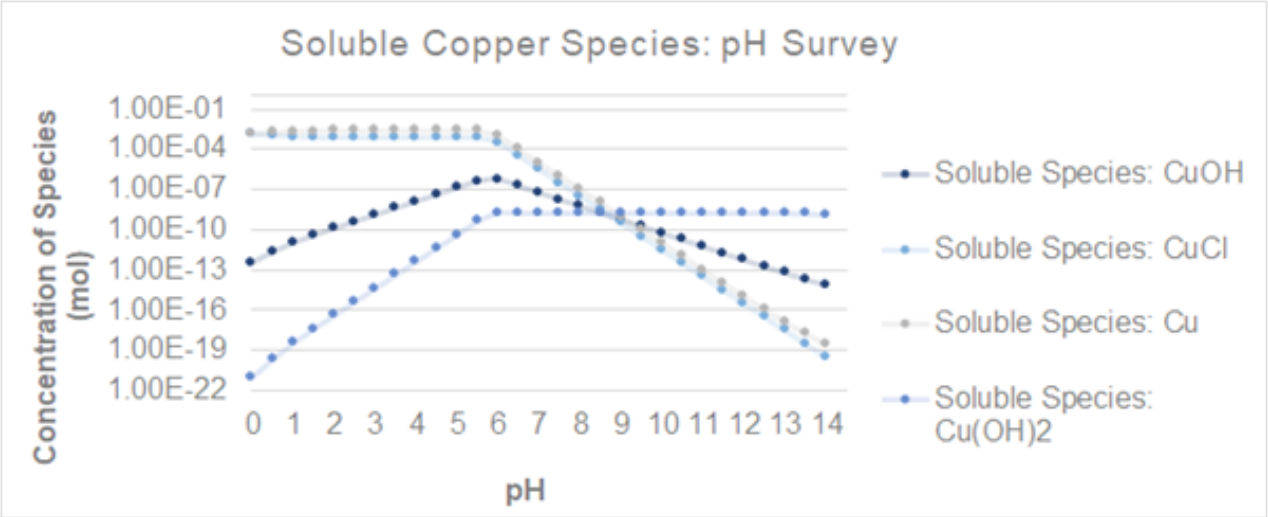

Figure S1: Soluble copper species present in the artificial wastewater containing a mixture of cations and anions